

## Diffusion Processes in the Sintering of Zirconia-Based Nanomaterials

Oksana Melikhova<sup>1,a</sup>, Jakub Čížek<sup>1,b</sup>, Ivan Procházka<sup>1,c</sup>, Wolfgang Anwand<sup>2,d</sup>,  
Tetyana E. Konstantinova<sup>3,e</sup>, Igor A. Danilenko<sup>3,e</sup>

<sup>1</sup>Faculty of Mathematics and Physics, Charles University in Prague,  
V Holešovičkách 2, CZ-180 00, Praha 8, Czech Republic

<sup>2</sup>Institut für Strahlenphysik, Helmholtz-Zentrum Dresden Rossendorf,  
Postfach 510119, D-01314 Dresden, Germany

<sup>3</sup>Donetsk Institute for Physics and Engineering named after O. O. Galkin of the NAS of Ukraine,  
Luxembourg Street 72, 83114 Donetsk, Ukraine

<sup>a</sup>oksivmel@yahoo.com (corresponding author), <sup>b</sup>jakub.cizek@mff.cuni.cz,  
<sup>c</sup>ivan.prochazka@mff.cuni.cz, <sup>d</sup>w.anwand@hzdr.de, <sup>e</sup>matscidep@aim.com

[Submitted: 7.7.2013; accepted: 4.9.2013]

**Keywords:** Yttria-stabilised zirconia, Nanopowders, Sintering, Porosity, Positron annihilation.

**Abstract.** In the present work, zirconia-based nanomaterials with various stabilizers were prepared by a co-precipitation technique. Defects in these nanomaterials were characterized by positron annihilation spectroscopy which is a non-destructive technique with a high sensitivity to open volume defects and atomic scale resolution. It was found that zirconia-based nanomaterials contain vacancies and also nano-scale and meso-scale pores. Diffusion processes which occur in the nanomaterials sintered at elevated temperatures were investigated by depth sensitive positron annihilation studies on a variable energy slow positron beam. It was found that sintering causes intensive grain growth and residual porosity is removed from samples by diffusion to the surface.

### Introduction

Zirconia ( $ZrO_2$ ) is an insulator which embodies a rare combination of advantageous thermal, electronic, mechanical and chemical properties [1]. The melting point of  $ZrO_2$  is as high as 2750 °C and it exhibits a low thermal conductivity. Likewise,  $ZrO_2$  is a very good high- $\kappa$  dielectric material showing a low electronic conductivity, but it is a good oxygen ionic conductor at increased temperatures. In addition,  $ZrO_2$  features a high hardness combined with reasonable fracture toughness and also good corrosion and wear resistance. Due to these properties,  $ZrO_2$  has become the base constituent of materials designed for a wide range of industrial applications, for example, as functional ceramics, refractory materials, solid oxide fuel cells, dental implants and abrasives.

Three  $ZrO_2$  polymorphs are known to exist. Such a polymorphism, however, considerably restricts exploitation of pure zirconia. This is because pure  $ZrO_2$ , which is monoclinic at room temperature, transforms to the denser tetragonal phase at  $\approx 1200^\circ\text{C}$  temperature. Such a transformation is accompanied with large volume changes and thus leads to creation of cracks within the  $ZrO_2$  structure. At temperatures higher than  $\approx 1380^\circ\text{C}$ , pure zirconia becomes cubic. Obviously, a stabilization of high-temperature  $ZrO_2$  phases is necessary to make full use of the advantageous zirconia features. Phase stabilization of zirconia can be achieved by an addition of a certain amount of the trivalent yttrium oxide ( $Y_2O_3$ , yttria) to form a solid solution in the  $ZrO_2$  lattice. Such a system is termed as yttria-stabilized zirconia (YSZ). Addition of  $\approx 3$  mol. % of the  $Y_2O_3$  stabilizer to zirconia stabilizes the tetragonal  $ZrO_2$  phase.

Nowadays, ternary zirconia-based solid oxide solutions, containing beside zirconia and yttria a third metal oxide ingredient, which is experiencing growing interest among researchers. Integration of another metal oxide into the YSZ system need not necessarily magnify a phase-stabilisation effect, but it may influence positively other characteristics of the material, e.g. mechanical properties, ionic conductivity, thermal stability and sintering temperature. Ternary YSZ containing

the trivalent chromium oxide ( $\text{Cr}_2\text{O}_3$ , chromia) is currently one of the most interesting zirconia-based ternary systems [2] because of the smaller ionic radius of  $\text{Cr}^{3+}$  compared to  $\text{Zr}^{4+}$  and a possible multiple Cr valence which may influence e.g. the diffusivity of Cr ions and/or grain growth.

Sintering is widely used for the manufacturing of ceramic materials from fine particle powders. The sintering procedure is always connected with mass transfer leading to grain growth and disappearance of pores. The key parameters controlling the sintering process are the sintering temperature,  $T_s$ , the mean particle size of initial powder, and also the diffusivity of the constituents.

In the present work, binary YSZ nanopowders and ternary YSZ nanopowders modified by addition of chromia were prepared and subsequently sintered at various temperatures. The diffusion processes during sintering of these nanopowders leading to removal of porosity and grain growth were investigated by variable energy slow positron annihilation spectroscopy (VEPAS) [3] which is a non-destructive technique with high sensitivity to open-volume defects.

## Experimental Details

Binary  $\text{ZrO}_2 + 3 \text{ mol. \% Y}_2\text{O}_3$  (Z3Y) and ternary  $\text{ZrO}_2 + 3 \text{ mol. \% Y}_2\text{O}_3 + 1 \text{ mol. \% Cr}_2\text{O}_3$  (Z3Y1Cr) nanopowders were prepared by the co-precipitation technique from salt-in-water solutions taken at stoichiometric compositions [2]. The initial nanopowders were calcined at  $500^\circ\text{C}/2 \text{ h}$  in air and pressed by uniaxial pressure of 500 MPa into pellets with diameter of  $\approx 10 \text{ mm}$  and thickness of  $\approx 5 \text{ mm}$ . The pellets were sintered at various temperatures gradually increasing from 600 to  $1350^\circ\text{C}$ . The sintering was always performed in air for 1 hour at each temperature.

VEPAS measurements were conducted using a magnetically guided variable energy slow positron beam SPONSOR [4]. The energy of incident positrons was varied in the range from 0.03 to 36 keV. Doppler broadening of the annihilation peak was measured by a HPGe detector with energy resolution of 1.03 keV at 511 keV. At least  $0.5 \times 10^6$  counts were accumulated in each spectra in the annihilation photo peak area. The  $S$  (sharpness) line shape parameter defined as the ratio of the central area of the annihilation peak to the net peak area was used for evaluation of Doppler broadening.

Positron lifetime (LT) measurements were carried out on a digital LT spectrometer [5] with excellent time resolution of 145 ps (FWHM for  $^{22}\text{Na}$ ). The positron source of about 1.3 MBq was made of carrier-free  $^{22}\text{Na}_2\text{CO}_3$  water solution (iThemba Laboratories) dried and sealed between 2  $\mu\text{m}$  mylar foils (DuPont). At least  $10^7$  annihilation events were accumulated in each LT spectrum.

## Results and Discussion

The TEM image of calcinated Z3Y powder prior to compaction into a pellet is shown in Fig. 1. The Z3Y powder consists of nanocrystalline particles with size 10-20 nm. A similar result was obtained also for the ternary nanopowder Z3Y1Cr but it exhibits a slightly smaller size of particles. X-ray diffraction investigations confirmed that calcined nanopowders as well as sintered ceramics exhibit the tetragonal zirconia structure. The mean size of crystallites determined using the Scherrer formula is  $(17.0 \pm 0.9) \text{ nm}$  and  $(13 \pm 1) \text{ nm}$  for Z3Y and Z3Y1Cr nanopowder, respectively.

The lifetimes  $\tau_i$  and relative intensities  $I_i$  of the exponential components resolved in LT spectra of compacted Z3Y and Z3Y1Cr nanopowders are listed in Table 1. In the compacted nanopowders all positrons annihilate either from trapped states at defects (saturated trapping) or form positronium (Ps), i.e. hydrogen-like bound state of electron and positron [6]. Since the size of crystallites is significantly smaller than the positron diffusion length in defect-free zirconia ( $\approx 200 \text{ nm}$ ) virtually all positrons diffuse to grain interfaces and are trapped at open-volume defects there. There are two kinds of positron traps at grain interfaces: (i) vacancy-like misfit distributed along grain boundaries and (ii) larger defects with size comparable to small vacancy clusters located at intersections of three or more grain boundaries (so-called triple points) [7]. The ternary Z3Y1Cr nanopowder contains similar kinds of defects but characterized by slightly higher lifetimes. This is due to Cr cations with a smaller radius than Zr ones segregating at grain boundaries and

surrounding the defects at grain boundaries. Moreover, because of the smaller crystallite size the ternary Z3Y1Cr nanopowder exhibits a higher  $I_2/I_1$  ratio than the binary Z3Y nanopowder [7].

**Table 1** Results of LT measurements: lifetimes  $\tau_i$  and relative intensities  $I_i$  of the components resolved in LT spectra. In fitting of LT spectrum of Z3Y nanopowder containing o-Ps contributions with lifetimes  $\tau_3$  and  $\tau_4$  a p-Ps contribution with lifetime of 125 ps and intensity  $1/3 (I_3 + I_4)$  was considered. Errors in the units of the last significant digit are given in parentheses.

Sample	$\tau_1$ (ps)	$I_1$ (%)	$\tau_2$ (ps)	$I_2$ (%)	$\tau_3$ (ns)	$I_3$ (%)	$\tau_4$ (ns)	$I_4$ (%)
Z3Y nanopowder	174(3)	27(2)	373(3)	63(2)	1.6(1)	1.4(1)	30(2)	5.9(3)
Z3Y1Cr nanopowder	190(4)	21(1)	387(2)	79(1)	-	-	-	-
Z3Y sintered $T_S = 1200^\circ\text{C}$	185(5)	98(1)	374(4)	2(1)	-	-	-	-
Z3Y1Cr sintered $T_S = 1200^\circ\text{C}$	180(4)	96(1)	380(4)	4(2)	-	-	-	-

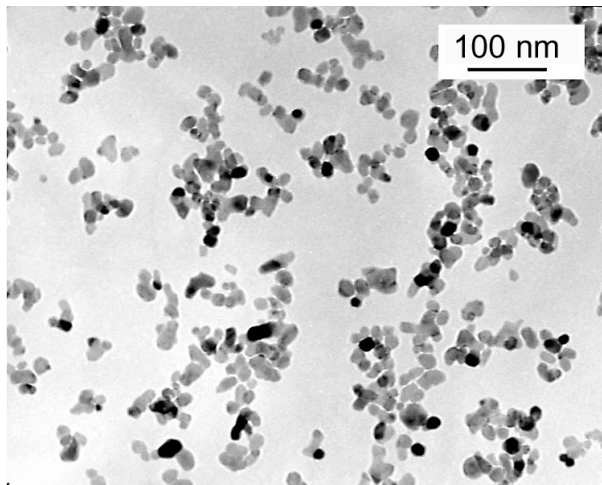


**Figure 1** TEM image of calcinated Z3Y nanopowder prior to compaction into pellet.

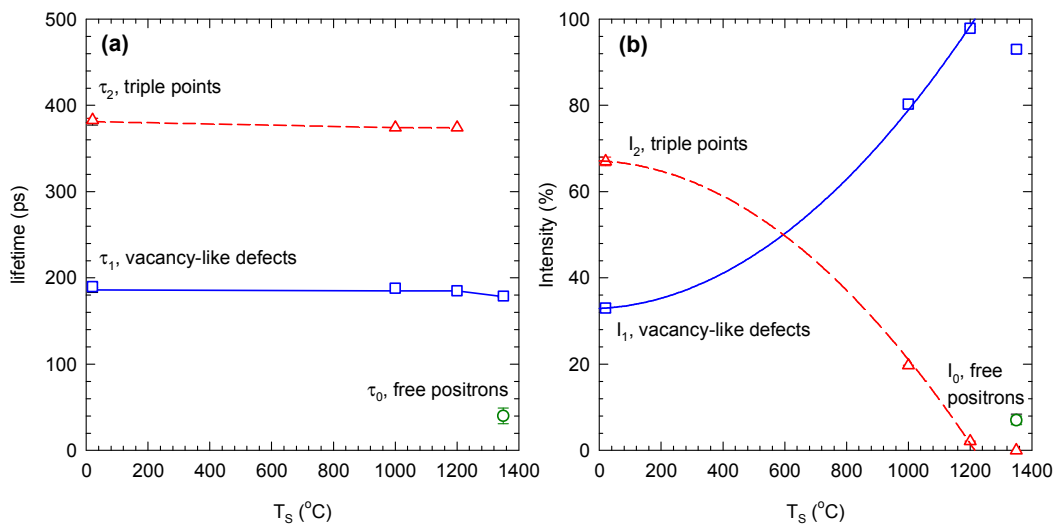


**Figure 2** Results of LT measurements of the binary Z3Y sample: lifetimes (a) and relative intensities (b) of the components resolved in LT spectra plotted as a function of the sintering temperature  $T_s$ . Open circles – free positron component; open squares – contribution of positrons trapped at vacancy-like defects; open triangles – positrons trapped at triple points.

One can see in Table 1 that a portion of  $\approx 7\%$  of positrons form Ps in binary Z3Y nanopowder. One can distinguish between singlet para-Ps (p-Ps) and triplet ortho-Ps (o-Ps) states which are formed in the ratio 1:3 [6]. The p-Ps decays quickly via self-annihilation – the lifetime of o-Ps in vacuum is 125 ps only. On the other hand, the self annihilation rate of o-Ps is roughly three orders

of magnitude lower compared to p-Ps and the lifetime of o-Ps in vacuum is 142 ns [6]. In solids o-Ps may annihilate with an electron of opposite spin from the surrounding media. This so-called pick-off annihilation significantly shortens the lifetime of o-Ps in solids [8-10]. The principal o-Ps component ( $\tau_4 \approx 30$  ns) detected in the binary YSZ nanopowder corresponds to mesopores with diameter of  $\approx 3$  nm estimated on the basis of the semi-empirical correlation between the o-Ps pick-off lifetime and the cavity size [8]. Since compacted nanopowders usually contain some residual porosity the principal o-Ps component can be attributed to o-Ps localized in big cavities between crystallites. The shorter and weaker o-Ps component with lifetime ( $\tau_3 \approx 1.6$  ns) can be attributed to smaller voids with diameter  $\approx 0.6$  nm estimated using the Tao-Eldrup model [9,10]. These sub-nanometer voids are probably situated at intersections of crystallite interfaces.

No Ps contribution was detected in the ternary Z3Y1Cr compacted nanopowders containing chromia since Ps formation is inhibited by paramagnetic  $\text{Cr}^{5+}$  cations acting as donors and introducing which free electrons at grain boundaries. As a consequence, any bound state between a positron and an electron localized at grain boundary is immediately broken in collisions with these quasi-free electrons introduced by  $\text{Cr}^{5+}$  ions [11].

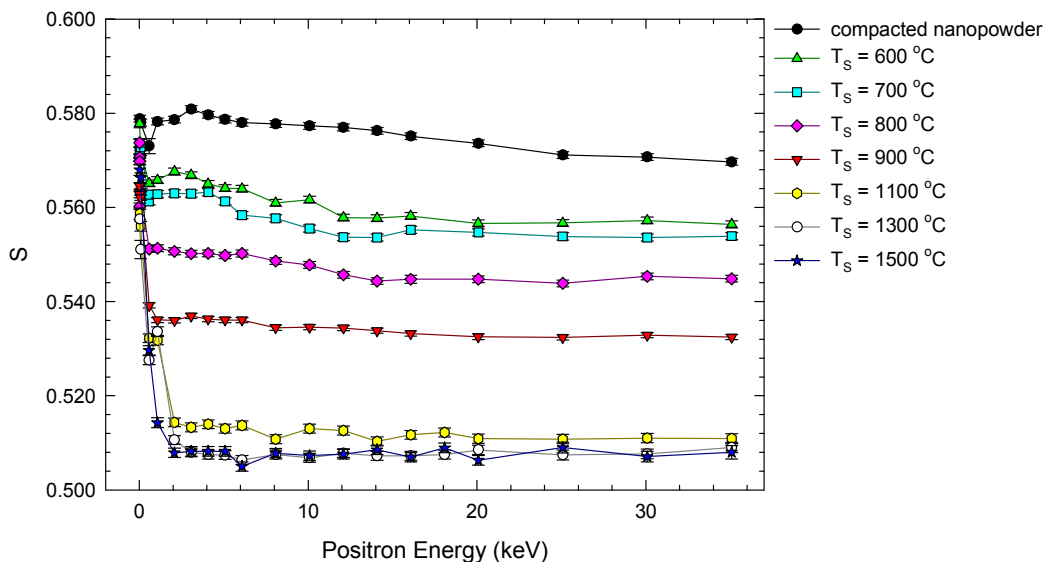


**Figure 3** The dependence of the  $S$  parameter on positron energy for the binary Z3Y nanopowder sintered at various temperatures  $T_s$ .

Removal of residual porosity during sintering requires mass transport which is limited by the diffusion of Zr cations to open pores, i.e. porosity is replaced by diffusing atoms and pushed towards the surface. To investigate this process depth sensitive VEPAS technique was employed. The dependences of the  $S$  parameter on positron energy for the binary Z3Y and the ternary Z3Y1Cr nanopowder sintered at various temperatures  $T_s$ , are plotted in Figs. 3 and 4, respectively. At very low energies almost all positrons annihilate at the surface. With increasing energy positrons penetrate deeper and deeper into the sample and the fraction of positron diffusing back to the surface decreases. This is reflected by a change of the  $S$  parameter from the surface value to the bulk value corresponding to the situation when all positrons are annihilated inside the sample. From inspection of Figs. 3 and 4 it becomes clear that the positron diffusion length in both nanopowders is very short and  $S$  reaches the bulk value already at the energy of  $\approx 2$  keV corresponding to the depth of  $\approx 20$  nm. This testifies that both nanopowders contain a very high concentration of defects leading to saturated positron trapping which is in accordance with LT investigations. Moreover, from comparison of Figs. 3 and 4 one can conclude that  $S$  parameters for the binary Z3Y nanopowder are higher than those for the ternary Z3Y1Cr sample. The enhanced  $S$  parameter in Z3Y is due to the contribution of p-Ps self-annihilation which has a very narrow momentum distribution and makes the annihilation peak narrower leading to increase of the  $S$  parameter [6].

The dependence of the  $S$  parameter on positron energy  $E$  for the binary Z3Y sample can be expressed as:

$$S(E) = S_{surf} F_{surf}(E) + S_{p-Ps} \frac{1}{4} F_{Ps}(E) + S_{o-Ps} \frac{3}{4} F_{Ps}(E) + S_V F_V(E) + S_T F_T(E), \quad (1)$$

where  $S_{surf}$ ,  $S_V$ ,  $S_T$ ,  $S_{p-Ps}$  and  $S_{o-Ps}$  stand for the  $S$  parameters for positrons annihilating at the surface, positrons trapped at vacancy-like defects, positrons trapped at triple points and positrons forming p-Ps and o-Ps, respectively. The relative fractions of positrons annihilated at various states always satisfy the normalization condition:

$$F_{surf}(E) + F_{Ps}(E) + F_V(E) + F_T(E) = 1. \quad (2)$$

The ternary Z3Y1Cr sample exhibits lower  $S$  parameters because the Ps contribution is absent (i.e.  $F_{Ps} \equiv 0$ ) since Ps formation is inhibited.

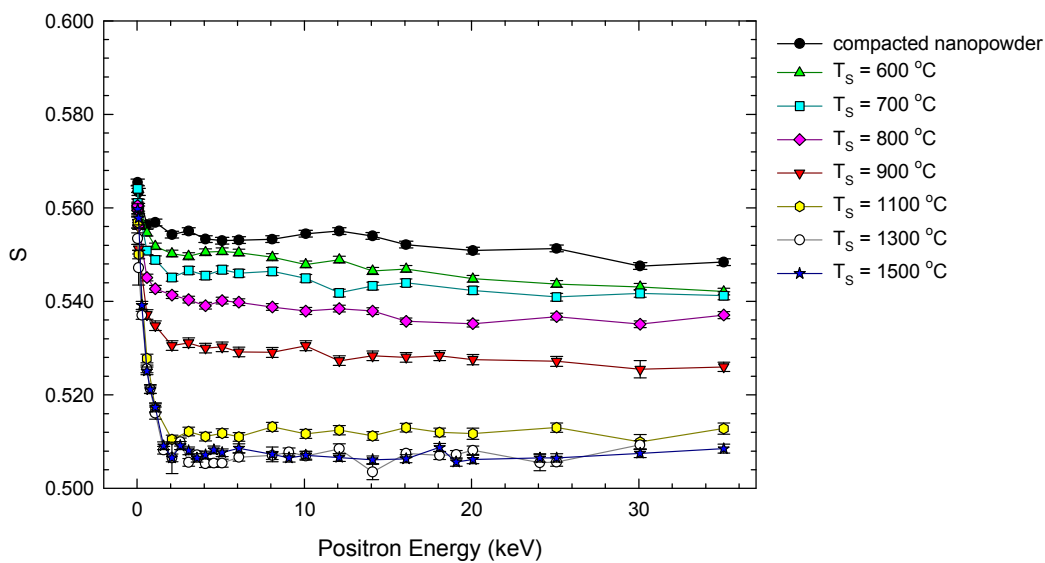


**Figure 4** The dependence of the  $S$  parameter on positron energy for the ternary Z3Y1Cr nanopowder sintered at various temperatures  $T_s$

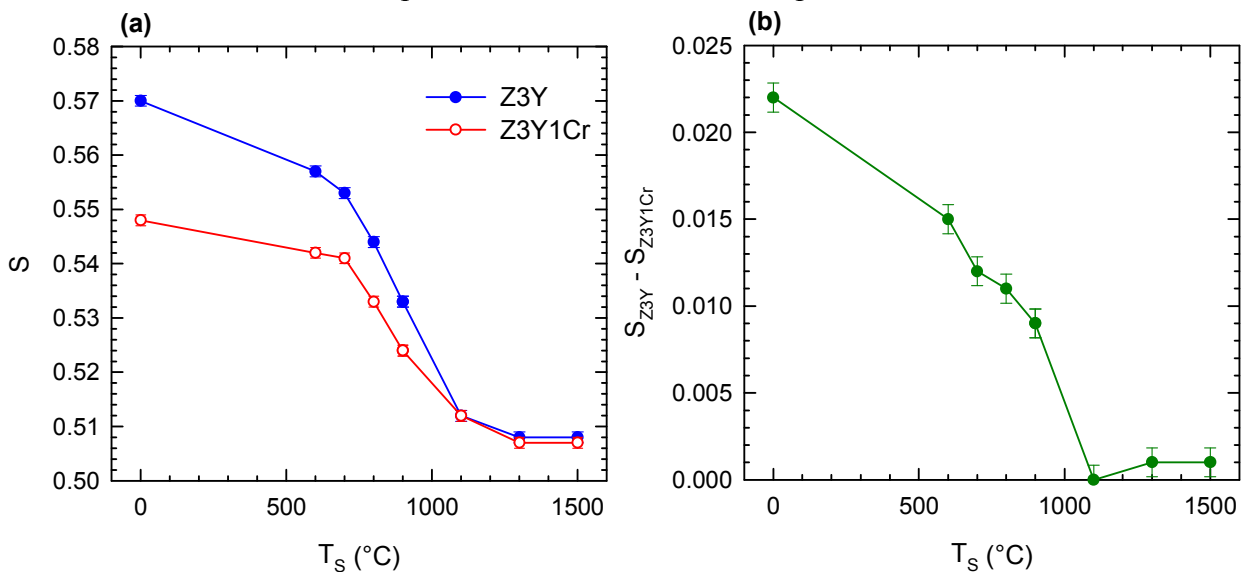


**Figure 5** (a) The dependence of the bulk  $S$  parameter on the sintering temperature; (b) the difference of the bulk  $S$  parameters for binary Z3Y and ternary Z3Y1Cr nanopowders plotted as a function of the sintering temperature  $T_s$ .

Fig. 5a shows the dependence of the bulk  $S$  parameter corresponding to positron energy  $E = 35$  keV on the sintering temperature for Z3Y and Z3Y1Cr. For positron energies high enough the fraction of positrons diffusing back to the surface becomes negligible, i.e.  $F_{surf} \equiv 0$ . Hence, the bulk  $S$  parameter for the binary Z3Y nanopowder can be written as:

$$S_{Z3Y} = S_{p-Ps} \frac{1}{4} F_{Ps} + S_{o-Ps} \frac{3}{4} F_{Ps} + S_V F_V + S_T F_T, \quad (3)$$

while for the ternary Z3Y1Cr nanopowder the bulk  $S$  parameter is given by a simpler expression:

$$S_{Z3Y1Cr} = S_V F_V + S_T F_T. \quad (4)$$

The fractions  $F_i$  in Eqs. (3) and (4) correspond to the energy  $E = 35$  keV. The characteristic  $S$  parameters for various positron states satisfy the following relation  $S_{p-Ps} > S_T > S_V$  and  $S_{o-Ps} \approx S_T$ . Hence, in the binary Z3Y nanopowder the bulk  $S$  parameter is determined by three contributions (i) positrons trapped at vacancy-like defects, (ii) positrons trapped at triple points and (iii) positrons forming Ps. The contribution (ii) depends on the volume fraction of grain boundaries, i.e. on the grain size, while the contribution (iii) depends on the concentration of porosity in the sample. In the Z3Y1Cr nanopowder Ps is not formed and the bulk  $S$  parameter depends on the grain size only.

Sintering leads to a decrease of the  $S$  parameter due to two processes: (1) grain growth which diminishes the concentration of triple points; (2) removal of porosity leading to disappearance of the Ps contribution. Both processes can be observed in the binary Z3Y sample, while in the ternary Z3Y1Cr only the process (1) can be observed due to lack of Ps contribution. Hence, the difference of the bulk  $S$  parameters  $S_{Z3Y} - S_{Z3Y1Cr}$  plotted in Fig. 5b is a measure of the porosity in the sample. Fig. 5b shows that the porosity is completely removed by sintering at 1000°C. Decrease of the  $S$  parameter during sintering at higher temperatures is caused solely by the grain growth.

## Summary

Compacted YSZ nanopowders contain vacancy-like misfit defects at grain boundaries, larger point defects located at triple points and meso-pores with a mean size of  $\approx 3$  nm. Two processes occur during sintering: (i) porosity is gradually removed by diffusion to surface leading to disappearance of Ps component, (ii) significant grain growth diminishes concentration of triple points. Both processes (i) and (ii) can be observed in the binary Z3Y, while in the ternary Z3Y1Cr sample formation of Ps is inhibited and only the process (i) can be observed. By comparison of results for samples one can conclude that porosity is removed completely by sintering at 1000°C.

## Acknowledgement

Financial support from the Czech Science Agency (project P108/11/1396) is highly acknowledged.

## References

- [1] A.G. Evans, R.M. Cannon, Overview no. 48: Toughening of brittle solids by martensitic transformations, *Acta Metall.* 34 (1986), 761-800.
- [2] I.A.Yashchishyn, A.M. Korduban, V.V. Trachevskiy, T.E. Konstantinova, I.A. Danilenko, G.K. Volkova, I.K. Nosolev, XPS and ESR spectroscopy of  $ZrO_2$ - $Y_2O_3$ - $Cr_2O_3$  nanopowders, *Functional Materials* 17 (2010), 306-310.
- [3] P.J. Schultz, K.G. Lynn, Interaction of positron beams with surfaces, thin films, and interfaces, *Rev. Mod. Phys.* 60 (1988), 701-779.

- 
- [4] W. Anwand, G. Brauer, M. Butterling, H.-R. Kissenger, A. Wagner, Design and Construction of a Slow Positron Beam for Solid and Surface Investigations, *Defect and Diffusion Forum* 331 (2012), 25-40.
- [5] F. Bečvář, J. Čížek, I. Procházka, J. Janotová, The asset of ultra-fast digitizers for positron-lifetime spectroscopy, *Nucl. Instr. Methods A* 539 (2005), 372-385.
- [6] O.E. Mogensen, *Positron Annihilation in Chemistry*, Springer-Verlag, Berlin, 1995.
- [7] J. Čížek, O. Melikhova, I. Procházka, J. Kuriplach, R. Kužel, G. Brauer, W. Anwand, T.E. Konstantinova, I.A. Danilenko, Defect studies of nanocrystalline zirconia powders and sintered ceramics, *Phys. Rev. B* 81 (2010), 024116-024135.
- [8] K. Ito, H. Nakanishi, Y. Ujihira, Extension of the Equation for the Annihilation Lifetime of ortho-Positronium at a Cavity Larger than 1 nm in Radius, *Journ. Chem. Phys. B* 103 (1999), 4555-4558.
- [9] S. Tao, Positronium Annihilation in Molecular Substances, *J. Chem. Phys.* 56 (1972), 5499-5510.
- [10] M. Eldrup, D. Lightbody, and J. Sherwood, The temperature dependence of positron lifetimes in solid pivalic acid, *Chemical Physics* 63 (1981), 51-58.
- [11] O. Melikhova, J. Čížek, I. Procházka, T.E. Konstantinova, I. A. Danilenko, Defect studies of yttria stabilized zirconia with chromia additive, *Physics Procedia* 35 (2012), 134-139.

**Journal of Nano Research Vol. 26**

10.4028/www.scientific.net/JNanoR.26

**Diffusion Processes in the Sintering of Zirconia-Based Nanomaterials**

10.4028/www.scientific.net/JNanoR.26.25